Technical Physics, 2025, Vol. 70, No. 3

09

Compact infrared radiation sources based on carbon nanotube films

© E.P. Kitsyuk,[1] A.V. Sysa,[1,2] A.V. Kuksin,[3] Yu.O. Vasilevskaya,[1] S.G. Moiseev,[2] Yu.P. Shaman[1,2]

[1]Scientific-Manufacturing Complex„"Technological Centre"„",
124498 Zelenograd, Moscow, Russia
[2]Ulyanovsk State University,
432017 Ulyanovsk, Russia
[3] Institute of Biomedical Systems, National Research University of Electronic Technology, „MIET",
124498 Zelenograd, Moscow, Russia
e-mail: kitsyuk.e@gmail.com

Received October 18, 2024
Revised October 18, 2024
Accepted October 18, 2024

Compact infrared radiation sources based on disordered carbon nanotube films were fabricated. The emission spectra of films based on single-walled (including those with characteristic metallic and semiconductor conductivity) and multi-walled carbon nanotubes were measured within the $3-10\,\mu$m wavelength interval at temperatures ranging from 150 °C to 400°C. The applicability of the manufactured radiation sources in measurements of transmission spectra of thin organic films is demonstrated.

Keywords: separation, laser cutting, carbon nanotubes, gas sensor, infrared radiation.

DOI: 10.61011/TP.2025.03.60860.328-24

Introduction

Gas sensors are used widely in various fields of science and technology [1–12], such as monitoring of harmful substances at industrial facilities [13,14], indoor air quality control [15,16], medical diagnostics [17], etc. The most efficient method for detection of various gases, including those hazardous to human health, in air is mid-infrared (IR) optical spectroscopy [18]. Non-dispersive IR sensors for gas environment monitoring offer high sensitivity and selectivity with respect to the detected gas mixture components and stability of parameters regardless of the concentration of oxygen and moisture in air throughout their entire service life. However, compact sources of IR $(3-12\,\mu\mathrm{m})$ radiation are needed for their efficient operation. A promising solution to this problem is the construction of IR emitters based on carbon nanotube (CNT) films with unique optical and electrophysical properties [19]. A coating of this kind may provide a near-unity light absorption coefficient, which is a fine approximation of a blackbody [20]. Therefore, in accordance with Kirchhoff's radiation law, the design of CNT-based emitters with a nanotube film acting as a heater and an emitting surface is promising in the context of fabrication of compact IR heaters, since this eliminates the need to form an additional layer with a high absorption coefficient on the surface of a MEMS (microelectromechanical system) heater [21,22]. The emissivity of an array of multi-walled carbon nanotubes (MWCNTs) deposited onto the surface of a MEMS heater was studied in [22]. The emissivity of single-walled carbon nanotube (SWCNT) networks was investigated in a similar manner [23]. In this regard, a comprehensive comparison of the emissivity of MWCNT and SWCNT films is an important research task.

1. Materials and methods

In order to compare the emission spectra of MWCNT and SWCNT films, IR emitters were formed on the surface of a mica substrate with the use of CNT layers of the corresponding types. Test structures were fabricated in a single technological cycle by forming the required topological CNT film pattern and subsequent nanosecond-laser cutting of the obtained structures into rectangular-shaped samples. The IR emitter samples were welded into a TO39-114 case for ease of measurement.

To analyze the effect of CNT fractions with metallic and/or semiconductor conductivity on the emission spectrum, commercial SWCNTs were separated via gel chromatography in accordance with the procedure outlined in [24]. This separation was performed for TUBALL 01RW03 SWCNTs (OCSiAl) with a diameter of $1.2-2$ nm and a length in excess of $5\,\mu$m.

Prior to separation, suspensions of nanotubes containing 20 mg of SWCNTs in 100 ml of a 1 % aqueous solution of sodium dodecyl sulfate (SDS) were prepared and processed with a homogenizer at an ultrasonic intensity of 50 W/cm^2 for 2 h in a temperature-controlled beaker at a temperature no higher than 15 °C. The obtained suspensions were centrifuged using a high-speed Avanti J-30I centrifuge (Beckman Coulter) for 60 min at 90 000 g. Following this, 3/4 of the CNT suspension (by volume) were retrieved from the test tubes and used for further separation of SWCNTs by conductivity type.

Sephacryl S-200 (10 ml) was used to fill the chromatographic column for the separation of CNTs. Prior to separation of SWCNTs by conductivity type, the filler was rinsed with a 1 % aqueous solution of SDS. A suspension

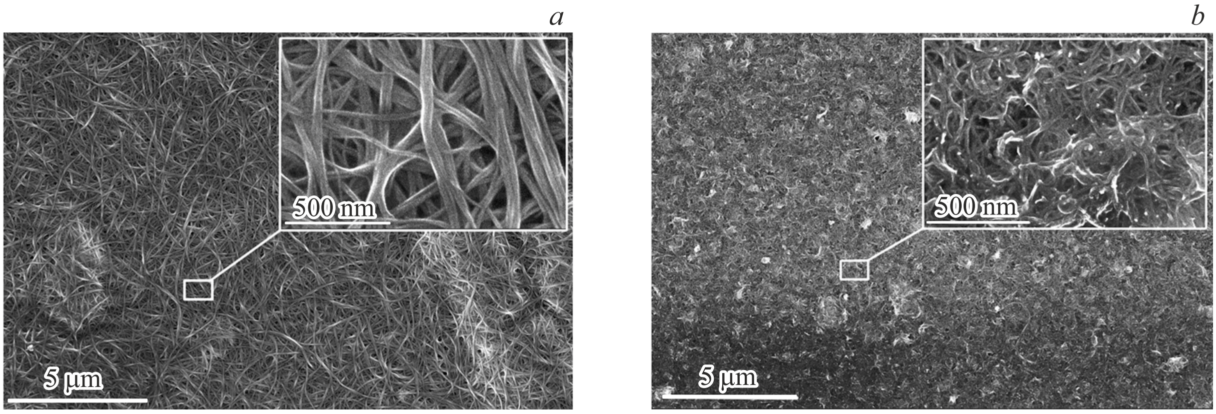

Figure 1. SEM images of films on the surface of mica. These films were formed from: *a* — original SWCNTs; *b* — MWCNTs.

of SWCNTs in 10 ml of a 1 % aqueous solution of SDS was then introduced into the chromatographic column. The SWCNT suspension filtered through the S-200 filler was collected, and the filler was rinsed with a 1 % aqueous solution of SDS to remove the residual suspension. The purified SWCNT suspension contained nanotubes of a predominantly metallic conductivity. CNTs were then eluted by rinsing the filler with a solution containing 1 % SDS and 1 % sodium deoxycholate (1 : 1 ratio). Filtered through S-200, this solution contained CNTs of a predominantly semiconductor conductivity.

Nanotubes synthesized using the method detailed in [25] were used to prepare a suspension of MWCNTs. According to scanning electron microscopy data, the characteristic diameter of the synthesized MWCNTs fell within the range from 6 to 30 nm. The obtained material was used to prepare a suspension of MWCNTs in a 1 % aqueous solution of SDS in accordance with the above procedure for SWCNTs.

SWCNT and MWCNT films were formed from the resulting suspensions by vacuum filtration. Membrane nitrocellulose filters with a diameter of 50 mm and a pore size of 0.2 μm were used as filter elements. The filter surface diameter was 40 mm. Prior to vacuum filtration, the absorbance of the CNT suspension used was measured at a wavelength of 400 nm in a cuvette with an optical path length of 10 mm. The absorbance of the suspension used was reduced to unity, which is equivalent to a suspension transmittance of 10 %. After the filtration process, the membrane filter with a CNT layer was introduced into a Petri dish filled with 50 ml of acetone. Following dissolution of the filter, 40 ml of acetone were removed with a syringe, 40 ml of pure acetone were added, and the solution was kept at rest for 20 min. This operation was repeated twice. At the next stage, 40 ml of acetone were removed with a syringe, and 100 ml of distilled water were added. SWCNT and MWCNT films were thus formed on the surface of the solution.

These CNT films were transferred by the aquaprint method from the solution surface to the surface of LF capacitor mica 50 μm in thickness. Mica was chosen as a substrate material due to the fact that it has a lower thermal conductivity coefficient (0.4–0.5 W/(m·K)) [26] than other dielectric substrates, such as sitall (0.8–2.5 W/(m·K)) or quartz (1.4 W/(m·K)) [27]; remains stable at temperatures up to 600 °C; has an absorbance at a wavelength of 1064 nm sufficient for laser cutting; and provides a proper minimum thickness of available substrates (30–60 μm). SEM images of the surface of films of the original SWCNTs and MWCNTs are shown in Figs. 1, *a* and *b*, respectively.

An ytterbium laser with a beam positioning system generating fundamental radiation with an IR wavelength of 1064 nm was used to form the required topological pattern on the CNT film surface. Laser removal of CNTs in specified regions of the film made it possible to form an array of rectangular CNT sections 2.5 × 4 mm in size. The distance between these rectangular regions was set to 1.1 and 2.2 mm in two orthogonal directions. The laser spot diameter in processing was ∼ 35 μm, the distance between the centers of adjacent spots was ∼ 17 μm, and the specified beam displacement rate was 240 mm/s. The laser was operated in pulsed mode with a pulse duration of 100 ns and a frequency of 30 kHz. The laser energy density was 70 J/cm^2. A total of 100 passes were performed. The entire 18.6 × 32.4 mm area was processed approximately in 2 min. For further assembly, the processed section together with the substrate was cut out using the same laser at a higher energy density of ∼ 100 J/cm^2.

Aluminum contact pads with a width of 3.2 mm were then formed by magnetron sputtering through a hard mask. The CNT film region not coated with aluminum was 2.5 × 3 mm in size. With the contact pads formed, working chips 6.2 × 3.6 mm in size were prepared by laser cutting at an energy density of ∼ 100 J/cm^2.

Individual chips were mounted in the TO39-114 case using aluminum wire 30 μm in thickness via ultrasonic welding (ES-4029). The welding pulse duration was 100 ms, the pressing force was 70 g, and the welding current was 62 mA. The procedure was performed in such a way that the substrate was mounted with an air gap and positioned at a distance of ∼ 2 mm from the base of the case. The external

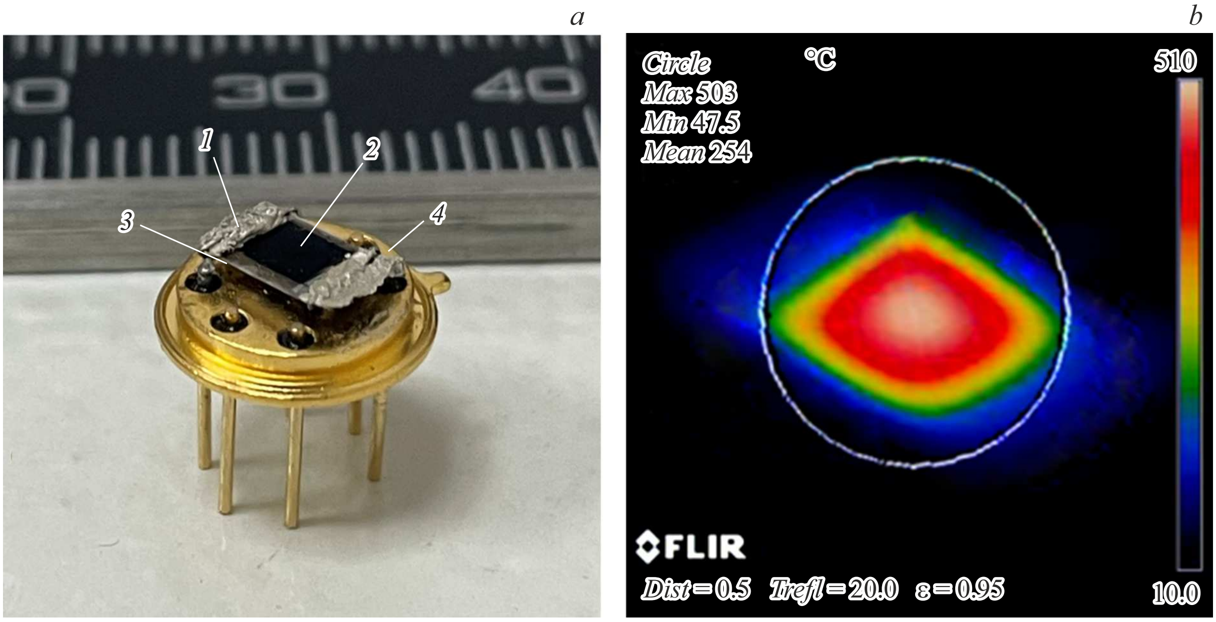

Figure 2. Compact IR radiation source based on CNT films: *a* — photographic image of the emitter (*1* — aluminum wire, *2* — working area of the CNT film, *3* — LF capacitor mica, and *4* — TO39-114 case); *b* — thermal image of the working area of the CNT film heated to 500°C.

view of the compact IR radiation source is presented in Fig. 2, *a*.

A supply voltage of 5−15 V from a B2912A precision source measurement unit (Agilent Technologies) was applied to the case terminals; the current was limited to 100 mA. The variation of temperature with voltage was monitored using a Flir P640 thermal imager within the range up to +500 °C. Figure 2, *b* shows the thermal image of the heated working area of the CNT film.

A spectral complex based on an iHR320 monochromator produced by HORIBA Scientific was used to measure the optical emission spectra of the fabricated IR emitter prototypes. A chopper modulating the optical signal with a frequency of 170 Hz was also applied in these experiments. The measurements were carried out within the 2−12 μm wavelength range at a pitch of 20 nm using a 300 gr/mm diffraction grating and an optical filter that restricted the propagation of radiation with a wavelength up to 1900 nm. A DSS-MCT(14)020L (mercury-cadmium-telluride) solid-state unit with nitrogen cooling served as a detector. The built-in preamplifier was disabled.

2. Results and discussion

Figure 3 shows the absorbance spectra of the original SWCNT suspension, the suspension of SWCNTs with semiconductor conductivity, the suspension of SWCNTs with metallic conductivity, and the MWCNT suspension after centrifugation.

The proportion content of SWCNTs with metallic and semiconductor conductivity in different suspensions was estimated in accordance with the procedure detailed in [28]. The areas of peak (M_1) within the 500−900 nm wavelength range for metallic SWCNTs and peak (E_{11}) within the 1300−2200 nm wavelength range for semiconductor SWCNTs were determined for this purpose. According to the formula given in [28], the fraction of SWCNTs with metallic conductivity may be calculated as follows:

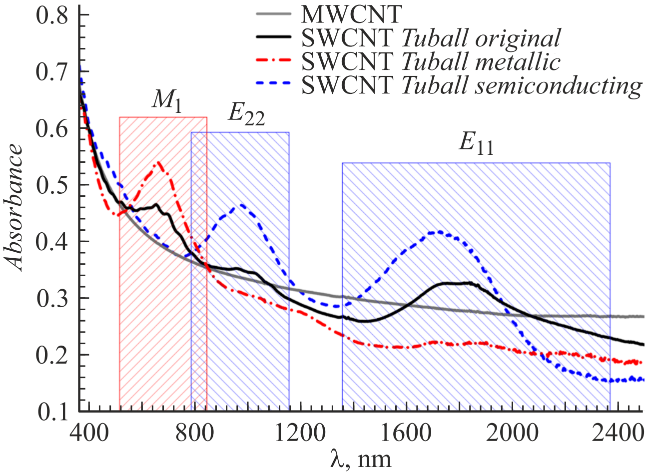

Figure 3. Absorbance spectra of different CNT suspensions.

$$R_M = \frac{1}{1 + \frac{E_{11}}{M_{11}}} \cdot 100\,\%. \qquad (1)$$

In the original suspension of SWCNTs, 62 % of nanotubes feature metallic conductivity, while the remaining 38 % have

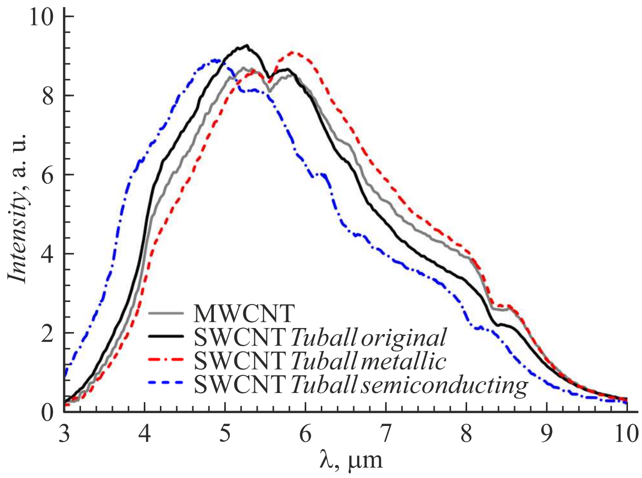

Figure 4. Emission spectra (normalized to the spectral sensitivity of the detector) of prototype IR emitters with CNTs of different conductivity types heated to a temperature of 250 °C.

semiconductor conductivity. The percentage of semiconductor SWCNTs in the suspension after elution increases to 97 %, and only 3 % of SWCNTs are metallic. In contrast, 92 % of SWCNTs in the suspension filtered through the S-200 filler feature metallic conductivity, and only 8 % are of the semiconductor type.

The emission spectra (normalized to the spectral sensitivity of the detector) of prototype IR emitters with different CNT films heated to 250 °C are shown in Fig. 4. The obtained results demonstrate that the emission spectra of films formed using the original SWCNTs and MWCNTs are similar. The emission maxima of films fabricated from SWCNTs with metallic or semiconductor conductivity are shifted. The emission maximum for the film formed from metallic SWCNTs is positioned close to 5.9 μm, and the emission of the film fabricated from predominantly semiconducting SWCNTs reaches its maximum around 4.9 μm. The observed shift of the emission intensity maximum of semiconductor SWCNT films may be attributed to plasmon resonance and an increase in the absorbance of films of SWCNTs with metallic conductivity at wavelengths greater than 4 μm relative to semiconductor SWCNT films [29]. A normalized sum of the emission spectra of films of SWCNTs with metallic and semiconductor conductivity provides a spectrum close to the emission spectrum of a film fabricated from the original SWCNTs.

The results of measurements of emission spectra at different temperatures of the film based on the original Tuball SWCNTs in air are shown in Fig. 5. As the temperature increases, an increase in emission intensity and a shift of the emission maximum toward shorter wavelengths are observed. This is consistent with Wien's displacement law.

The time dependences of electrophysical parameters of the prototype IR emitter based on the original SWCNT film at a heater temperature of 400 °C are presented in Fig. 6. The voltage first decreases from 9.4 to 9.2 V, but then increases monotonically to 9.6 V. This supply voltage reduction at the initial stage of operation of the IR emitter may be attributed to a decrease in resistance of the SWCNT film as a result of removal of functional groups, which were formed in the process of acid treatment of SWCNTs for elimination of catalytic impurities, from the CNT surface [30,31]. The subsequent increase in supply voltage is attributable to the deterioration of the electrical contact between CNTs and the aluminum electrodes due to aluminum oxidation [32], since, according to thermal analysis data, CNTs remain stable in an oxygen-containing environment through to 500 °C (inset in Fig. 6). The SWCNT film mass loss during heating is associated with the removal of functional groups from the SWCNT walls [31]. To suppress the influence of contact resistance between the metal electrode and CNTs on the stability of the IR emitter, one needs to use protective coatings preventing metal oxidation or use metals that are less susceptible to oxidation under heating.

The feasibility of application of a CNT film as a heater and an emitting surface for spectral studies in the IR range is demonstrated below. The designed prototype IR radiation source was used to measure the transmission spectrum of nitrocellulose within the 3–12 μm wavelength range. The supply voltage of the IR emitter based on the original Tuball SWCNT film was 9.7 V, the current was 106 mA, and the IR emitter temperature determined from thermal imaging data was 400 °C. The transmission spectrum is shown in Fig. 7. The transmission spectrum of nitrocellulose measured with a Nicolet iS50 IR Fourier spectrometer is also presented in Fig. 7. A comparison of these spectra reveals that they match completely in the number of peaks and their position within the 4–9 μm wavelength range. The positions of peaks within the 9–12 μm wavelength range deviate by no more than 120 nm.

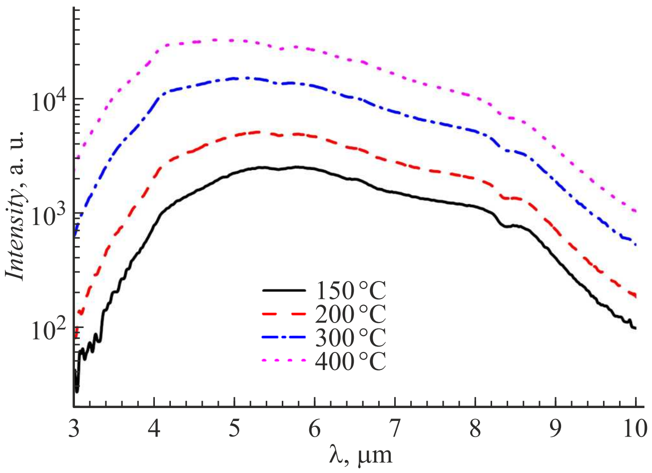

Figure 5. Emission spectra of the original Tuball SWCNT film at different temperatures in air.

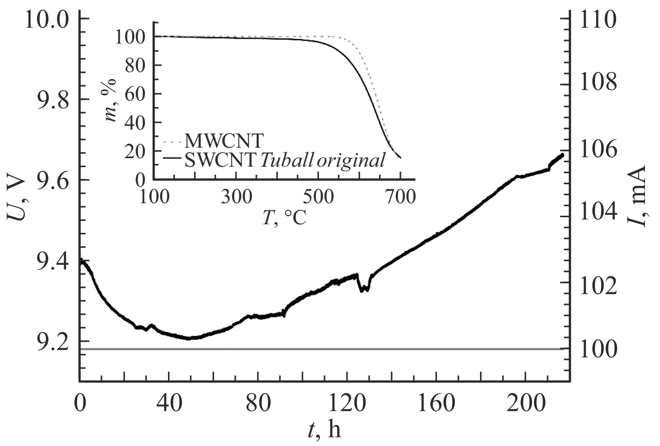

Figure 6. Time dependence of the current and voltage of the prototype IR emitter based on a Tuball SWCNT film. The temperature dependence of the CNT film mass measured in the process of heating in an oxygen-containing environment is shown in the inset.

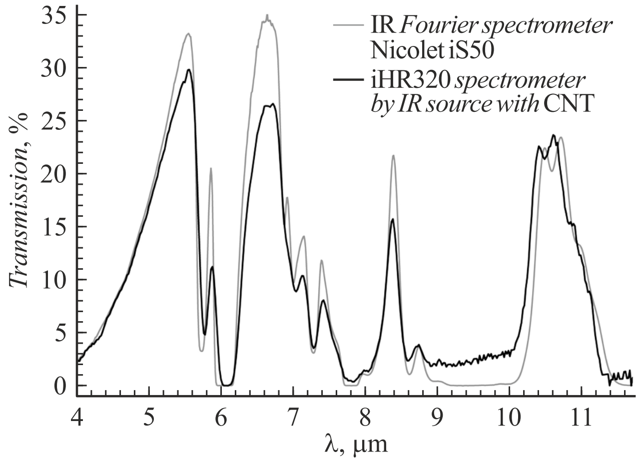

Figure 7. Transmission spectrum of a nitrocellulose film.

Conclusion

An original design of an IR radiation source with operating wavelengths ranging from 3 to 12 μm and a CNT film used as a heater and an emitting surface was proposed. The analysis of emission of the manufactured IR emitters based on MWCNT and SWCNT films with different conductivity types revealed that the emission spectra of MWCNTs and the original SWCNTs are similar; however, the emission intensity maxima of films fabricated from SWCNTs with semiconductor and metallic conductivity types are shifted in opposite directions by up to 1000 nm relative to the positions of peaks in the emission spectrum of the original nanotubes. The measurements of temporal variation of electrophysical parameters verified the long-term applicability of the manufactured IR emitters at a film heating temperature up to 400 °C, provided that a reliable contact is formed between the metal electrode and the CNT film through the use of corrosion-resistant metals and/or protective coatings that suppress the influence of the ambient environment.

Funding

Engineering work on the infrared radiation source, the SWCNT application process design, and measurements of the emission spectra and the electrophysical parameters of the fabricated structures were supported financially by the Russian Science Foundation, project No. 23-19-00880. The technology for separating CNTs by conductivity type was developed with support from project FNRM-2024-0001.

Conflict of interest

The authors declare that they have no conflict of interest.

References

[1] M.K. Rabchinskii, V.V. Sysoev, O.E. Glukhova, M. Brzhezinskaya, D.Yu. Stolyarova, A.S. Varezhnikov, M.A. Solomatin, P.V. Barkov, D.A. Kirilenko, S.I. Pavlov, M.V. Baidakova, V.V. Shnitov, N.S. Struchkov, D.Yu. Nefedov, A.O. Antonenko, P. Cai, Z. Liu, P.N. Brunkov. Adv. Mater. Technol., **7** (7), 2101250 (2022). DOI: 10.1002/admt.202101250

[2] Z. Meng, J. Zhuang, X. Xu, W. Hao, S.X. Dou, Y. Du. Adv. Mater. Interfaces, **5**, 1800749 (2018). DOI: 10.1002/admi.201800749

[3] D. Fan, X. Yang, J. Liu, P. Zhou, X. Zhang. Compos. Commun., **27**, 100887 (2021). DOI: 10.1016/j.coco.2021.100887

[4] X. Yang, J. Liu, D. Fan, J. Cao, X. Huang, Z. Zheng, X. Zhang. Chem. Eng. J., 389, **124448** (2020). DOI: 10.1016/j.cej.2020.124448

[5] W.C. Tan, K.-W. Ang. Adv. Electron. Mater., **7**, 2001071 (2021). DOI: 10.1002/admt.202101250

[6] S. Orzechowska, A. Mazurek, R. Swisłocka, W. Lewandowski. Materials, **13**, 80 (2020). DOI: 10.3390/ma13010080

[7] C. Anichini, W. Czepa, D. Pakulski, A. Aliprandi, A. Ciesielski, P. Samori. Chem. Soc. Rev., **47**, 4860 (2018). DOI: 10.1039/C8CS00417J

[8] F. Schedin, A.K. Geim, S.V. Morozov, E.W. Hill, P. Blake, M.I. Katsnelson, K.S. Novoselov. Nat. Mater., **6**, 652 (2007). DOI: 10.1038/nmat1967

[9] K. Deshmukh, T. Kovarik, S.K.K. Pasha. Coord. Chem. Rev., **424**, 213514 (2020). DOI: 10.1016/j.ccr.2020.213514

[10] M. Donarelli, L. Ottaviano. Sensors, **18**, 3638 (2018). DOI: 10.3390/s18113638

[11] N. Joshi, T. Hayasaka, Y. Liu, H. Liu, O.N. Oliveira Jr., L. Lin. Microchim. Acta, **185**, 213 (2018). DOI: 10.1007/s00604-018-2750-5

[12] R.A. Potyrailo, V.M. Mirsky. Chem. Inform., **39** (19), (2008). DOI: 10.1002/chin.200819271

[13] C.S. Goldenstein, R.M. Spearrin, J.B. Jeffries, R.K. Hanson. Progr. Energy Combustion Sci., **60**, 132 (2017). DOI: 10.1016/j.pecs.2016.12.002

[14] U. Willer, M. Saraji, A. Khorsandi, P. Geiser, W. Schade. Opt. Lasers Engineer., **44** (7), 699 (2006). DOI: 10.1016/j.optlaseng.2005.04.015

[15] A. Schieweck, E. Uhde, T. Salthammer, L.C. Salthammer, L. Morawska, M. Mazaheri, P. Kumar. Renewable and Sustainable Energy Rev., **94**, 705 (2018). DOI: 10.1016/j.rser.2018.05.057

[16] A. Ortiz Perez, B. Bierer, L. Scholz, J. Wöllenstein, S. Palzer. Sensors, **18** (12), 43445 (2018). DOI: 10.3390/s18124345

[17] M. Metsälä. J. Breath Research, **12** (2), 027104 (2018). DOI: 10.1088/1752-7163/aa8a31

[18] J. Hodgkinson, R.P. Tatam. Measurement Sci. Technol., **24** (1), 012004 (2012). DOI: 10.1088/0957-0233/24/1/012004

[19] H.-S.P. Wong, D. Akinwande. *Carbon Nanotube and Graphene Device Physics* (Cambridge University Press, 2010), DOI: 10.1017/CBO9780511778124

[20] Z.-P. Yang, L. Ci, J.A. Bur, S.-Y. Lin, P.M. Ajayan. Nano Lett., **8** (2), 446 (2008). DOI: 10.1021/nl072369t

[21] N. Li, H. Yuan, L. Xu, Y. Zeng, B. Qiang, Q.J. Wang, S. Zheng, H. Cai, L.Y.T. Lee, N. Singh, D. Zhao. Opt. Express, **29** (12), 19084 (2021). DOI: 10.1364/oe.422204

[22] D. Popa, R. Hopper, S.Z. Ali, M.T. Cole, Y. Fan, V.-P. Veigang-Radulescu, R. Chikkaraddy, J. Nallala, Y. Xing, J. Alexander-Webber, S. Hofmann, A. De Luca, J.W. Gardner, F. Udrea. Scientific Reports, **11** (1), 22915 (2021). DOI: 10.1038/s41598-021-02121-5

[23] L. Lai, P. Liu, D. Zhou, Q. Li, S. Fan, W. Lu. Adv. Functional Mater., **33** (4), 2208891 (2023). DOI: 10.1002/adfm.202208891

[24] H. Liu, D. Nishide, T. Tanaka, H. Kataura. Nature Commun., **2** (1), 309 (2011). DOI: 10.1038/ncomms1313

[25] A.A. Pavlov, A.V. Sysa, Yu.P. Shaman, M.I. Bazarova, I.M. Gavrilin, A.A. Polokhin. Russ. Microelectron., **46** (2), 82 (2017). DOI: 10.1134/s1063739717020068

[26] N.P. Bogorodskii, V.V. Pasynkov, B.M. Tareev. *Elektrotekhnicheskie materialy* (Energoatomizdat, L., 1985) (in Russian).

[27] L.A. Novitskii, I.G. Kozhevnikov. *Teplofizicheskie svoistva materialov pri nizkikh temperaturakh* (Mashinostroenie, M.,1975) (in Russian).

[28] Y. Miyata, K. Yanagi, Y. Maniwa, H. Kataura. J. Phys. Chem. C, **112** (34), 13187 (2008). DOI: 10.1021/jp804006f

[29] K. Oi, J. Komoto, T. Kawai, Y. Nonoguchi. Synthetic Metals, **282**, 116958 (2021). DOI: 10.1016/j.synthmet.2021.116958

[30] M.R. Predtechenskiy, A.A. Khasin, A.E. Bezrodny, O.F. Bobrenok, D.Yu. Dubov, V.E. Muradyan, V.O. Saik, S.N. Smirnov. Carbon Trends, **8**, 100175 (2022). DOI: 10.1016/j.cartre.2022.100175

[31] A. Yaya, C.P. Ewels, Ph. Wagner, I. Suarez-Martinez, A.G. Tekley, L.R. Jensen. Europ. Phys. J. Appl. Phys., **54** (1), 10401 (2011). DOI: 10.1051/epjap/2011100482

[32] L.P.H. Jeurgens, W.G. Sloof, F.D. Tichelaar, E.J. Mittemeijer. Thin Solid Films, **418** (2), 89 (2002). DOI: 10.1016/s0040-6090(02)00787-3

Translated by D.Safin